PVDF–TiO_2 Composite Hollow Fiber Ultrafiltration Membranes Prepared by TiO_2 Sol–Gel Method and Blending Method

Li-Yun Yu,[1,2] Hong-Mei Shen,[2] Zhen-Liang Xu[1,2]

[1]*Key Laboratory for Ultrafine Materials of the Ministry of Education, East China University of Science and Technology (ECUST), Shanghai 200237, China*
[2]*Membrane Science and Engineering R&D Lab, Chemical Engineering Research Center, ECUST, Shanghai 200237, China*

Received 5 January 2008; accepted 18 December 2008
DOI 10.1002/app.29886
Published online 17 April 2009 in Wiley InterScience (www.interscience.wiley.com).

ABSTRACT: Organic–inorganic polyvinylidene fluoride (PVDF)–titanium dioxide (TiO_2) composite hollow fiber ultrafiltration (UF) membranes were prepared by TiO_2 sol–gel method and blending method, respectively. The membranes were characterized in terms of microstructure, hydrophilicity, permeation performance, thermal stability, and mechanical strength. The experimental results indicated that PVDF–TiO_2 composite UF membranes exhibited significant differences in surface properties and intrinsic properties because of the addition of inorganic particles. The TiO_2 particles improved the membrane strength and thermal stability of PVDF–TiO_2 composite UF membranes. In particular, hydrophilicity and permeability increased dramatically with the increase of TiO_2, whereas the retention property of UF membranes was nearly unchanged. However, high TiO_2 concentration induced the aggregation of particles, resulting in the decline of hydrophilicity and permeability. Compared with PVDF–TiO_2 composite hollow fiber UF membranes prepared by TiO_2 blending method, PVDF–TiO_2 composite hollow fiber UF membranes prepared by TiO_2 sol–gel method formed a dispersed inorganic network, and the stronger interaction between inorganic network and polymeric chains led to TiO_2 particles being uniformly dispersed in UF membranes.
 J Appl Polym Sci 113: 1763–1772, 2009

Key words: polyvinylidene fluoride; titanium dioxide; sol–gel method; blending method; hollow fiber UF membrane

INTRODUCTION

Currently, polymers are still the main materials in membrane technology, with the advantages of good membrane forming ability, flexibility, and low cost. However, limited chemical, mechanical, and thermal resistance restricts the application of polymer materials. As reported in the literature,[1,2] ceramic membranes have higher thermal and chemical resistance as well as longer lifetime, but they are still expensive and brittle, with poor membrane-forming ability. Composite materials could combine basic properties of organic and inorganic materials and offer specific advantages for the preparation of artificial membranes with excellent separation performances, good thermal and chemical resistance, adaptability to harsh environments, and membrane-forming ability.[3–6] Therefore, organic–inorganic composite materials as new membrane materials have increasingly attracted attention.

Polyvinylidene fluoride (PVDF) is one of the most extensively applied membrane materials in the industry because of outstanding antioxidation activity, strong thermal and hydrolytic stability, as well as good mechanical and membrane-forming properties. However, its hydrophobic nature, which often results in severe membrane fouling and decline of permeability, has been a barrier to its application in water treatment.[7] Many studies have attempted to improve the hydrophilicity of PVDF membranes using various techniques, including physical blending, chemical grafting, and surface modifications.[8] Among these methods, blending with inorganic materials has much interest because of the materials' convenient operations, mild conditions, and good and stable performances.[9]

The sol–gel technique is one of the most extensively applied methods for the preparation of organic–inorganic materials; it allows the formation of inorganic frameworks under mild conditions and the incorporation of minerals into polymers, resulting in increased chemical, mechanical, and thermal stability without obviously decreasing the properties

Correspondence to: Z.-L. Xu (chemxuzl@ecust.edu.cn).
Contract grant sponsor: National Key Fundamental Research Development Plan ("973" Plan); contract grant number: 2003CB615705.

Journal of Applied Polymer Science, Vol. 113, 1763–1772 (2009)

TABLE I
TiO_2 Concentration of PVDF-TiO_2 (Sol–Gel Method) Dopes

Sample number	TiO_2 concentration (wt %)[a]
M-1	0
M-2	0.25
M-3	0.5
M-4	0.75
M-5	1.0
M-6	1.25
M-7	1.5
M-8	2.0
M-9	3.0
M-10	4.0

[a] Calculated TiO_2 concentration (wt %) of PVDF-TiO_2 dopes under the assumption that the sol–gel reaction was completed.

of the polymers.[10–12] Furthermore, the remaining hydrogen bond clusters at the surfaces of the materials after the sol–gel reaction improve membrane hydrophilicity and enhance the stability of the composite material.[13–18]

Inorganic materials that could be blended with PVDF include titanium dioxide (TiO_2),[19] silica (SiO_2),[20] zirconium dioxide (ZrO_2),[21] alumina (Al_2O_3),[8,22] and some small molecule inorganic salts such as lithium salts.[23] In the present study, PVDF UF membranes were modified by inorganic TiO_2 particles. TiO_2 as an active material has many advantages, such as innocuity, resisting and decomposing bacteria, UV resistance, and superhydrophilicity.[24]

The aim of this work was to prepare organic–inorganic PVDF–TiO_2 composite hollow fiber UF membranes with high hydrophilicity, permeability, mechanical strength, and thermal stability by sol–gel method and blending method. The preparation of PVDF–TiO_2 composite UF membranes with finely dispersed TiO_2 in the polymer matrix was discussed. The effects of adding TiO_2 particles on membrane properties were investigated on the basis of permeation, hydrophilicity, thermal analysis, and mechanical properties, as well as the microstructures and titanium distribution in membranes. Furthermore, effects of TiO_2 particles on the structure and performances of the PVDF–TiO_2 composite hollow fiber UF membranes prepared by sol–gel method and blending method were compared.

EXPERIMENTAL

Materials

Polyvinylidene fluoride (PVDF) (Solef 1015) and titanium dioxide (TiO_2) particles (25 nm in size, P25) were purchased from Solvay Advanced Polymers (Alpharetta, GA) and Evonik Degussa (Dusseldorf, Germany), respectively. Polyvinylpyrrolidone (PVP, K30), *N*,*N*-dimethylacetamide (DMAc), *N*-methyl-2-pyrrolidinone (NMP), and tetrabutyltitanate [$Ti(OBu)_4$] were all obtained from the Shanghai Chemical Reagent Company (Shanghai, China). Acetic acid and hydrochloric acid (HCl, 36–38%) were of analytical grade (from the Beijing Chemical Reagent Company, Beijing, China) and used as received. Lysozyme (M_w = 14,400) was purchased from Shanghai Bio Life Sci and Tech.

TiO_2 sol preparation

Acetic acid (1.0 mL) and 10.0 mL $Ti(OBu)_4$ were added to 10.0 mL NMP with stirring (Solution A). Hydrochloric acid (0.3 mL) and 2 mL deionized water were added to another 10 mL NMP (Solution B). Then, Solution B was added dropwise to Solution A with vigorous stirring for 2 h at 25°C. After mixing uniformly, a stable, transparent, and flaxen TiO_2 solution was obtained with pH 4.0 adjusted by hydrochloric acid.

Preparation of hollow fiber membranes and modules

TiO_2 solution or TiO_2 particles were added to the dope of DMAc and NMP ($V_{DMAC} : V_{NMP} = 4 : 1$) containing 18 wt % PVDF and 5 wt % additive PVP (K30) with constant stirring at 25°C for 24 h to get a homogenous PVDF–TiO_2 dope for spinning.

PVDF–TiO_2 hollow fiber UF membranes were spun by the wet-spinning method at 25°C, as described elsewhere.[25–28] Dope and bore fluid solution passed through the spinneret at the pressure of N_2 and constant-flow pump, respectively. The dopes were first kept in the tank overnight to degas before spinning. TiO_2 concentration (wt %) of PVDF–TiO_2 dopes is summarized in Table I (sol–gel method) and Table II (blending method). The fabricated hollow fiber membranes were stored in a water bath for 24 h to remove residual solvents and were then immersed in a tank containing 50 wt % glycerol

TABLE II
TiO_2 Concentration of PVDF-TiO_2 (Blending Method) Dopes

Sample number	TiO_2 concentration (wt %)
M-11	0.5
M-12	0.75
M-13	1.0
M-14	1.5
M-15	2.0
M-16	3.0
M-17	4.0
M-18	5.0

aqueous solution for 24 h to prevent the collapse of porous structures. The membranes were air dried at room temperature to make test modules.

Membrane modules were prepared to quantitatively test the hollow fiber separation performances in terms of permeation flux and rejection. The hollow fiber UF membrane modules were self prepared (outside feeding, which meant that the feed solution was entered into the external surface of the hollow fiber membrane, and the permeated solution was flowed out of the internal surface of the hollow fiber membrane under certain pressure difference), and the external and inner diameters of the pipeline were 0.8 and 0.6 cm, respectively. Four hollow fibers with an effective length of 22.5 cm and total effective membrane area of 4.24×10^{-3} m^2 were composed into a module. The shell sides of the two ends of the bundles were glued onto two stainless steel tees using a normal-setting epoxy resin. These modules were left overnight for curing before being tested. To eliminate the effect of the residual glycerol on module performance, each module was immersed in water for 24 h and run in the test system for 1 h under a pressure of 0.1 MPa before sample collection.

Membrane characterizations

Morphology observation

The morphology of PVDF–TiO_2 hollow fiber UF membranes was examined by scanning electron microscopy (SEM) (Model JSM-6360 LV, JEOL, Japan). The fibers were first immersed in liquid nitrogen for a few minutes, then broken and deposited on a copper holder. All samples were coated with gold under vacuum before testing. For the same samples of SEM, the linescan spectrum of energy dispersion of X-ray (EDX; EDAX Falcon) was applied to detect the particle distribution profile on the surface of the PVDF–TiO_2 hollow fiber UF membranes.

X-ray diffraction analysis

The membrane X-ray diffraction (XRD) patterns were recorded on a D/max-rB diffractometer (Rigaku, Japan) equipped with graphite monochromated Cu Kα radiation ($\lambda = 0.15405$ nm) operated at 50 mA and 50 kV from 10° to 80°.

Hydrophilicity, porosity, and pore size measurement

The contact angle (θ) between water and the membrane surface was measured to evaluate the membrane hydrophilicity using a JC2000A Contact Angle Meter produced by Shanghai Zhongcheng Digital Equipment (Shanghai, China). To minimize experimental error, the contact angles were measured five times for each sample and then averaged.

The membrane porosity ε (%) was defined as the volume of the pores divided by the total volume of the porous membrane. It could usually be determined by gravimetric method, determining the weight of liquid (here pure water) contained in the membrane pores.[29]

$$\varepsilon = \frac{(w_1 - w_2)/d_w}{(w_1 - w_2)/d_w + w_2/d_p} \times 100\% \quad (1)$$

where w_1 was the weight of the wet membrane (g), w_2 was the weight of the dry membrane (g), d_w was the pure water density (0.998 g cm^{-3}) and d_p was the polymer density (1.765 g cm^{-3}).

Mean pore radius r_m (μm) was determined by the filtration velocity method. According to the Guerout–Elford–Ferry equation, r_m could be calculated[30]:

$$r_m = \sqrt{\frac{(2.9 - 1.75\varepsilon) \times 8\eta l Q}{\varepsilon \times A \times \Delta P}} \quad (2)$$

where η was the water viscosity (8.9×10^{-4} Pa s), l was the membrane thickness (m) (namely the differential value between external radius and inner radius of the hollow fiber membrane), Q was the volume of the permeate water per unit time (m^3 s^{-1}), A was the effective area of the membrane (m^2), and ΔP was the operational pressure (0.1 MPa).

Maximum pore size R_{max} (μm) could be obtained by the bubble point method. According to Laplace's equation, maximum pore size could be calculated[31] as follows:

$$R_{max} = \frac{2\sigma \cos\theta}{P} \quad (3)$$

where σ was the surface tension of water (71.96×10^{-3} N m^{-1}), θ was the contact angle of water to membrane (°), and P was the minimum bubble point pressure (Pa).

Permeation flux and rejection measurement

The permeation flux and rejection of PVDF–TiO_2 hollow fiber UF membranes were measured by UF experimental equipment, as shown in Figure 1. The rejection test was carried out with an aqueous solution of lysozyme (300 mg L^{-1}). All experiments were conducted at 25°C and under the feed pressure of 0.1 MPa. The newly prepared PVDF–TiO_2 hollow fiber membranes were prepressured at 0.1 MPa using pure water for 1 h before measurement, then the pure water permeation (J_w) was measured, and, finally, the permeation flux (J_L) and rejection (R) for the lysozyme solution were measured.

The concentrations of lysozyme in the permeate and feed were determined by a UV-spectrophotometer

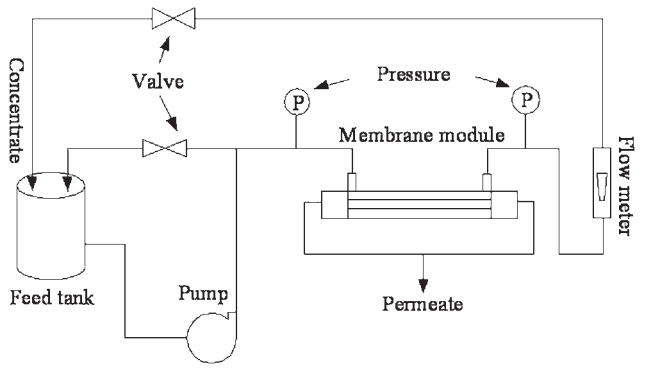

Figure 1 Schematic diagram for UF experimental equipment.

(Shimadzu UV-3000, Japan). The permeation flux (J) and rejection (R) were defined as formulae (4) and (5), respectively.

$$J = \frac{Q}{A \times T} \tag{4}$$

$$R = \left(1 - \frac{C_P}{C_F}\right) \times 100\% \tag{5}$$

where J was the permeation flux of the membrane for pure water or lysozyme solution (L h^{-1} m^{-2}), Q was the volume of the permeate pure water or lysozyme solution (L), A was the effective area of the membrane (m^2), and T was the permeation time (h). R was the rejection to lysozyme (%), and C_P and C_F were the permeate and feed concentration (wt %), respectively.

A primary reason for flux decline during the initial period of the membrane separation process was concentration polarization of solute on the membrane surface. As reported in the literature,[32] concentration polarization was more severe with a decreasing Reynolds number R_e, as a lower R_e would result in a lower mass transfer coefficient and, correspondingly, more serious concentration polarization. Therefore, it was indicated that R_e could partly imply the degree of concentration polarization.

$$R_e = \frac{d_e u \rho}{\mu} \tag{6}$$

$$d_e = 4 \times \frac{S}{\prod} = 4 \times \left(\frac{\frac{\pi}{4}D^2 - n \times \frac{\pi}{4}d^2}{\pi D + n \times \pi d}\right) = \frac{D^2 - nd^2}{D + nd} \tag{7}$$

where d_e was the equivalent diameters (m), u was lysozyme solution mean velocity under the feed pressure of 0.1 MPa (2.82 m s^{-1}), ρ was lysozyme solution density (0.999 g cm^{-3}), μ was lysozyme solution viscosity (9.1×10^{-4} Pa s), S was the cross section area of the pipeline (m^2), Π was the wetting perimeter (m), D was the inner diameter of the pipeline (0.6 cm), d was the external diameter of the hollow fiber membrane (1.5 mm), and n was the number of hollow fibers in each membrane module (n was 4, as mentioned earlier).

Thermal analysis

The thermal stability of composite membranes was evaluated by thermal gravitational analysis (TGA) (TA SDT-Q600). The TGA measurements were carried out under nitrogen atmosphere at a heating rate of 10°C min^{-1} from 50 to 800°C. Differential scanning calorimetry (DSC, Perkin-Elmer Pyris Diamond) measurements were performed on the composite membranes from 50 to 300°C at a heating rate of 10°C min^{-1}. The first scan was run to 300°C for 10°C min^{-1} to destroy any initial thermal history, and then the sample was cooled to 50°C to start the second scan.

Mechanical stability testing

Tensile strength and elongation percent of the composite membranes were measured by material test machine (Shimadzu) at loading velocity of 50 mm min^{-1}. The report values were measured five times for each sample and then averaged.

RESULTS AND DISCUSSION

Membrane morphology

The morphology of PVDF and PVDF–TiO_2 UF membranes was observed by SEM. The cross-section morphologies of UF membranes are shown in Figure 2, which illustrates that the macrovoids grew and became run-through at lower TiO_2 concentration (M-1, M-3, and M-11) and then were suppressed or disappeared at higher TiO_2 concentration, (M-5, M-7, M-13, and M-14). Moreover, with the increase in TiO_2 concentration, the cross-sectional morphologies of PVDF–TiO_2 UF membranes changed from finger-like to sponge-like structures. As seen in Figure 3 and Table III, the addition of fewer TiO_2 particles resulted in the increase of mean pore size compared with PVDF membranes. However, higher TiO_2 concentration induced an aggregate phenomenon, and there were aggregates of TiO_2 particles adsorbing or embedding on the surface of PVDF–TiO_2 composite membranes (such as M-7 and M-14 in Fig. 3), thereby blocking the pores and decreasing the mean pore size.

These experimental results indicated that the addition of TiO_2 particles had a big effect on membrane structure. The increase in the viscosity of the dope because of the addition of TiO_2 particles slowed down the exchange rate of solvent/nonsolvent and tended to a delayed demixing process, resulting in

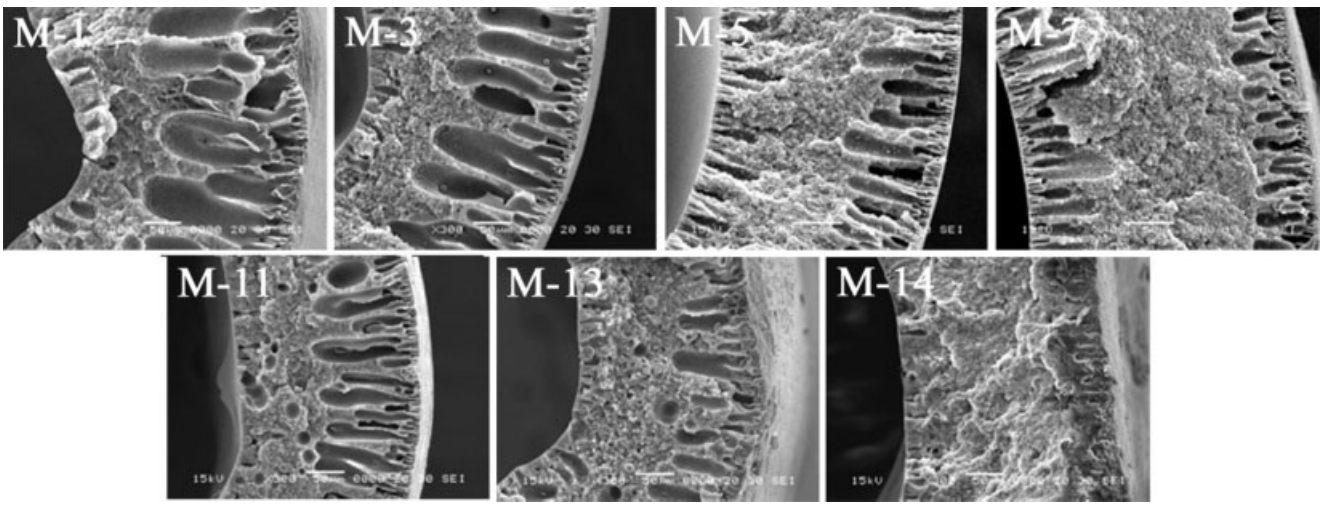

Figure 2 Cross-section morphologies of M-1, M-3, M-5, M-7, M-11, M-13, and M-14.

the suppression of macrovoids. In keeping with to the hypothesis of McKelvey and Koros,[33] macrovoids were initiated by nucleation of the polymer-lean phase just beneath the skinlayer, and their growth depended on the difference between the indiffusion rate of nonsolvent to dope and the diffusion rate of the solvent to coagulation bath. This rate difference induced a nonsolvent concentration gradient in the dope, which formed a drive force to cause the macrovoids growth. With the increase in dope viscosity induced by addition of TiO_2 particles, the diffusion of nonsolvent slowed down greatly, and nonsolvent concentration decreased. Consequently, the formation or the growth of macrovoids in membranes was suppressed. Therefore, it was concluded that the mechanical properties of composite membranes were altered by the addition of TiO_2.

EDX analyses

EDX was applied to investigate the distribution of the TiO_2 particles on the surface of the membranes. The EDX titanium linescan spectra of the PVDF–TiO_2 membranes for M-5 and M-13 are shown in Figure 4. When the additional amount of TiO_2 particles was 1 wt % by the sol–gel method (M-5), the particles were distributed uniformly on the surface, and the mean weight percent of Ti was 2.59 wt %. However, when the additional amount of TiO_2 particles was 1 wt % by the blending method (M-13),

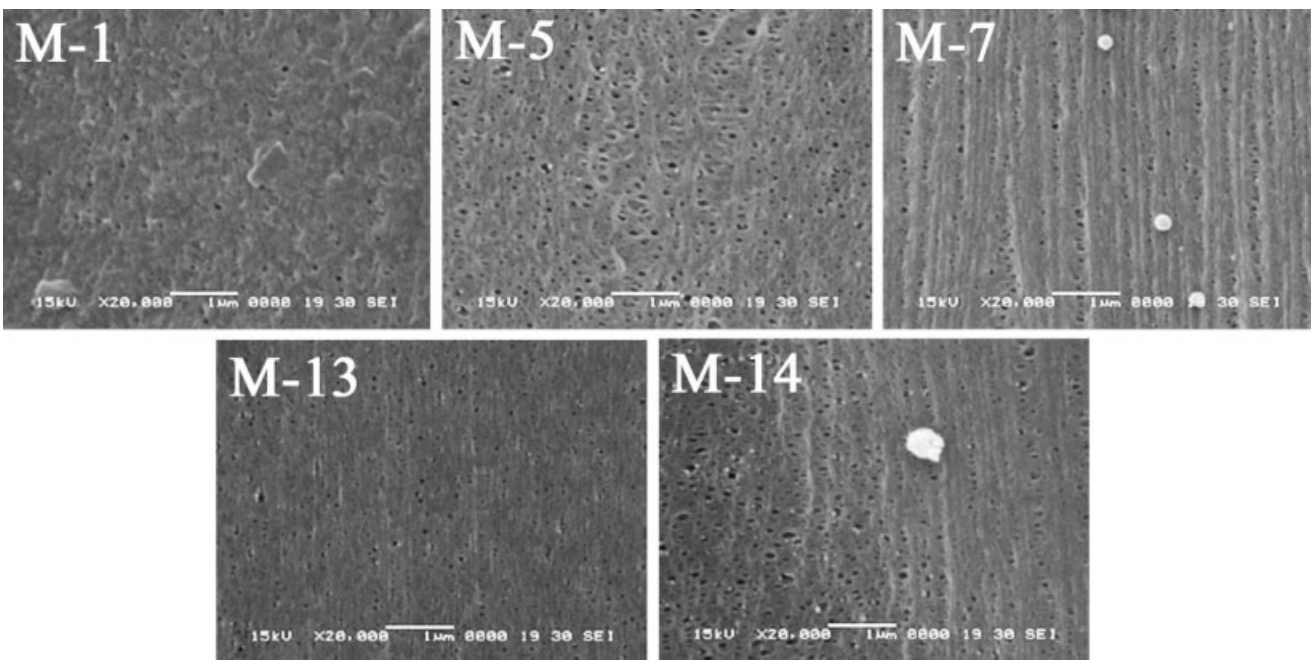

Figure 3 Surface morphologies of M-1, M-5, M-7, M-13, and M-14.

TABLE III
Contact Angle and Pore Structure Parameters of PVDF–TiO_2 Membranes with Different TiO_2 Concentrations

Sample no.	TiO_2 concentration (wt %)	Contact angle θ (°)	Porosity ε (%)	Pore size	
				r_m (μm)	R_{max} (μm)
M-1	0	79.13	79.03	0.061	0.272
M-2	0.25	51.68	70.34	0.076	0.196
M-3	0.5	40.35	64.75	0.090	0.203
M-4	0.75	38.13	62.51	0.103	0.217
M-5	1.0	34.91	60.39	0.115	0.224
M-6	1.25	42.69	63.01	0.100	0.243
M-7	1.5	53.25	64.09	0.093	0.265
M-8	2.0	65.28	66.12	0.083	0.291
M-9	3.0	70.64	74.23	0.080	0.334
M-10	4.0	72.86	76.75	0.079	0.387
M-11	0.5	64.55	73.56	0.067	0.212
M-12	0.75	61.73	69.08	0.075	0.235
M-13	1.0	58.36	61.54	0.089	0.269
M-14	1.5	63.54	62.35	0.078	0.287
M-15	2.0	68.87	64.87	0.071	0.307
M-16	3.0	69.87	68.93	0.065	0.359
M-17	4.0	72.38	72.51	0.055	0.412
M-18	5.0	73.84	77.39	0.051	0.487

the EDX spectra showed heterogeneous distribution of Ti, which was caused by the aggregation of TiO_2 particles. At the same time, the mean weight percent of Ti was 1.98 wt % because of aggregates of TiO_2 particles packed by polymers or embedded in the membrane matrix. As the EDX spectra showed, TiO_2 particles were distributed more uniformly by the sol–gel method (M-5) than by the blending method (M-13).

XRD analyses

Figure 5 shows the XRD diffraction patterns of TiO_2 particles by sol–gel method, PVDF membrane, and PVDF–TiO_2 composite membrane made from M-5. The pattern of TiO_2 crystal powder had three crystalline characteristic peaks at 2θ of 25.3°, 37.82°, and 48.04°, which agreed with the literature,[24] and the pattern of composite membrane also had three crystalline characteristic peaks at 2θ of 25.42°, 37.9°, and 48.14° that was analogous with the characteristic peaks of TiO_2 crystal powder. This indicated that tetrabutyl titanate had formed TiO_2 crystals through a hydrolytic reaction during the preparation of the PVDF–TiO_2 composite membrane. Moreover, the peaks at 18.46° and 20.24° in Figure 5(b) corresponded to the diffractions in the 020 and 021 planes, respectively, all characteristic of α phase PVDF. The peak at 20.68° in Figure 5(c) refers to the

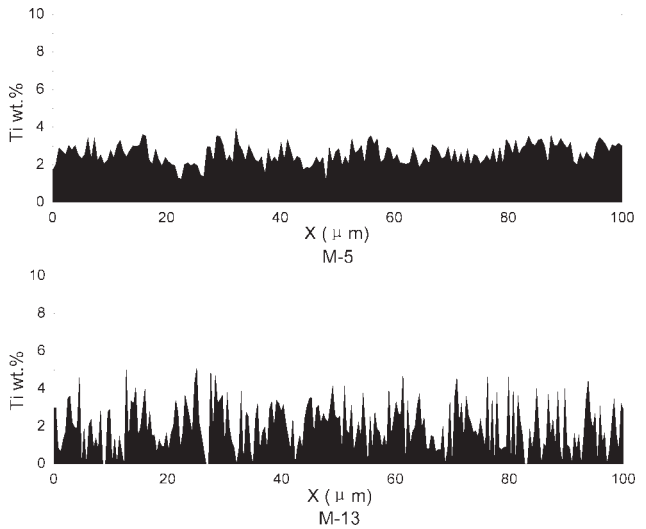

Figure 4 EDX titanium line scanning spectra for the surface of the PVDF–TiO_2 hollow fiber membranes made from M-5 and M-13.

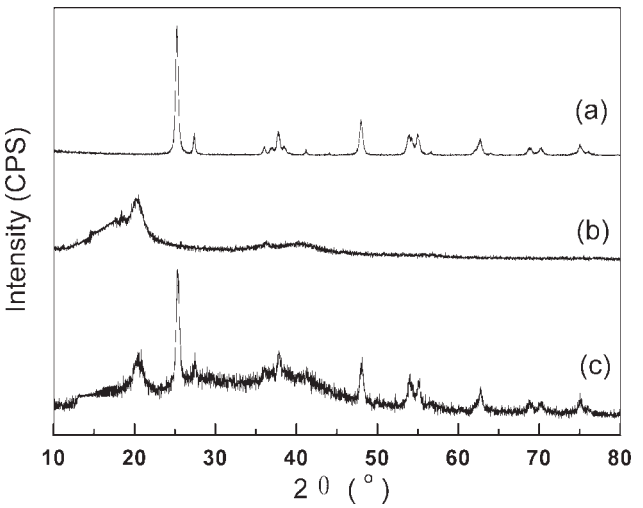

Figure 5 X-ray diffraction patterns of TiO_2 powder by sol–gel (a), PVDF membrane (b), and PVDF-TiO_2 membrane for M-5 (c).

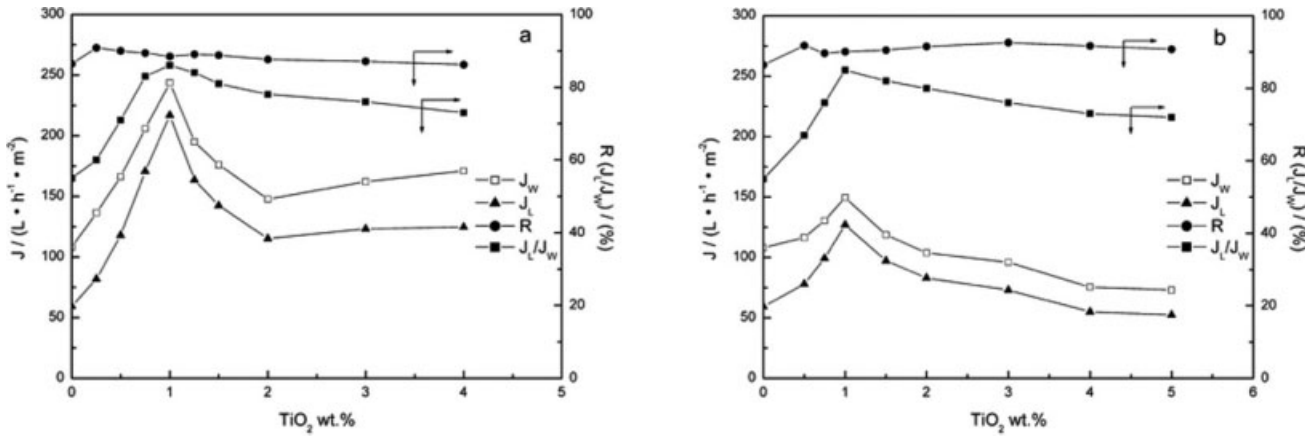

Figure 6 Curves of J_w and J_L, retention (R), and the ratio (J_L/J_w) of PVDF–TiO_2 composite membranes by sol–gel method (a) and blending method (b) as a function of TiO_2 concentration.

sum of the diffraction in the 110 and 200 planes, characteristic of β-phase PVDF.[34] It appears that TiO_2 crystals had distributed to the membrane matrix and influenced the PVDF crystal structure (transition from α crystalline phase to β-crystalline phase) in the composite membrane.

Hydrophilicity, porosity, and pore size of membranes

Surface hydrophilicity was one of the important properties of membranes which could affect the flux and antifouling ability of membrane. In general, hydrophilicity was evaluated by contact angle with water, and membrane surface hydrophilicity was higher when its contact angle was smaller. The contact angle data of PVDF–TiO_2 composite membranes with different TiO_2 concentrations (Table III) showed that the membrane hydrophilicity improved with the addition of TiO_2 particles by both sol–gel method and blending method. This was because the hydrophilic TiO_2 particles, which contained hydroxyl groups adsorbed on the membrane surface, were responsible for increased hydrophilicity.[22] However, the contact angle increased when the TiO_2 concentration was more than 1 wt % because of particle aggregates, resulting in the decrease of effective hydrophilic area and hydroxyl group number.[8] The results demonstrated that adding TiO_2 particles into PVDF polymer by sol–gel method could improve its hydrophilicity, and the affect was more obvious than blending method.

The porosity and pore size information of the prepared membranes are listed in Table III. It was shown that the porosity decreased with the increase of TiO_2 concentration ($\leq$ 1 wt %) and then increased at the higher TiO_2 concentration ($>$ 1 wt %). The addition of TiO_2 particles led to a denser cross-sectional structure, thereby inducing the decrease of porosity at the lower TiO_2 concentration ($\leq$ 1 wt %). Adding more TiO_2 particles ($>$ 1 wt %) enhanced the formation of larger pores in the vicinity of TiO_2 aggregates as well as of defects in the membrane, thus increasing porosity. In Table III, the mean pore size first increased and then decreased. In fact, there existed interfacial stresses between the polymer and TiO_2 particles, which finally formed interfacial pores because of the shrinkage of the organic phase during the demixing process, increasing the mean pore size with the addition of the lower amount of TiO_2 particles. However, the higher TiO_2 particle concentration blocked the pores and induced the formation of denser a cross-sectional structure, consequently decreasing the mean pore size. As shown in Table III, the maximum pore size decreased first and then increased, because the lower amount of TiO_2 particles could suppress defects in the membrane, whereas when the amount of TiO_2 added was larger, the aggregation of TiO_2 particles produced a considerable number of larger pores, mostly formed in the vicinity of TiO_2 aggregates, decreasing the bubble point pressure and increasing the maximum pore size.

Permeation flux and rejection of membranes

The influences of TiO_2 concentration on permeability and retention were investigated through UF experiments. Figure 6, shows that the membrane permeability first increased and then decreased with the increase in TiO_2 concentration, with a peak value 244 L h^{-1} m^{-2} of pure water and 217 L h^{-1} m^{-2} of lysozyme solution when TiO_2 concentration was 1 wt % in Figure 6(a), and a maximum value 150 L h^{-1} m^{-2} of pure water and 127 L h^{-1} m^{-2} of lysozyme solution when TiO_2 concentration was 1 wt % in Figure 6(b). The increase in the membrane hydrophilicity and mean pore size with lower TiO_2 concentration ($\leq$ 1 wt %) (Table III) could attract water

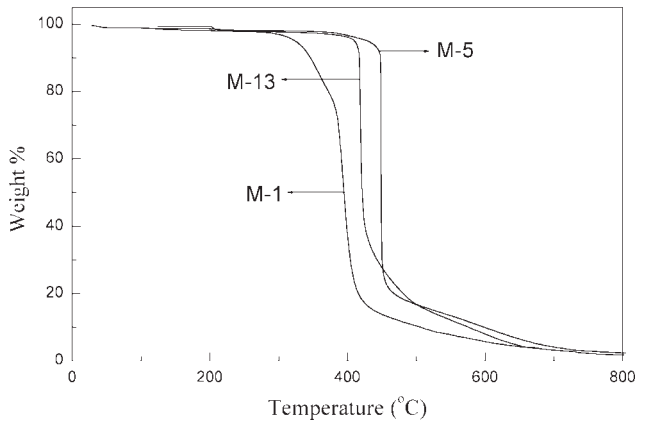

Figure 7 TG curves of PVDF–TiO_2 membranes: M-1, T_d 338.67°C; M-5, T_d 401.7°C; M-13, T_d 369.73°C.

molecules inside the membrane matrix, facilitating their penetration through the membrane and enhancing permeability. However, higher TiO_2 concentration (> 1 wt %) resulted in the formation of a highly viscous dope. This slowed down the formation process of PVDF–TiO_2 composite membranes and produced a compact network sublayer, shown in Figure 2, containing considerable TiO_2 particles blocking membrane pores, thereby decreasing the hydrophilicity and mean pore size and resulting in decrease in permeability. Furthermore, in Figure 6, the retention of composite membrane to lysozyme was almost unchanged compared to the PVDF membrane, owing to the balance between maximum pore size increase in Table III and denser cross-section structure with the increase of TiO_2 concentration seen in Figure 2. Therefore, PVDF–TiO_2 composite UF membranes with appropriate TiO_2 particles possessed superior permeability and nearly unchanged retention. Moreover, the testing results demonstrated that permeability of PVDF–TiO_2 membranes by the sol–gel method was better than blending method. It could be interpreted that adding TiO_2 particles into PVDF polymer by the sol–gel method could improve its hydrophilicity and pore size, and the effect was more obvious than by the blending method.

When the feed was a lysozyme solution (300 mg L^{-1}) at 25°C under the feed pressure of 0.1 MPa, Reynolds number, R_e could be calculated according to formulae (6) and (7), and the obtained R_e value was 6966. As reported in the literature,[32] it usually presented turbulent flow as $R_e > 4000$. Higher shear velocity in turbulent flow was beneficial to remove solutes and grains from the membrane surface, leading to a decline in the degree of concentration polarization and membrane fouling.

The antifouling properties of PVDF–TiO_2 composite hollow fiber UF membranes could be evaluated by the ratio of lysozyme solution flux (J_L) to pure water flux (J_w).[7] For the higher antifouling UF membrane, the addition of lysozyme in the feed solution would cause a little flux loss and the ratio (J_L/J_w) would be higher. As shown in Figure 6, the ratio (J_L/J_w) first increased and then decreased slightly with the increase in TiO_2 concentration. The membrane surface hydrophilicity improved significantly as the hydrophilic TiO_2 particles on the membrane surface reduced the interaction between the contaminants and the membrane surface, effectively improving the antifouling properties. However, with the dope containing greater than 1 wt % TiO_2 particles, the ratio (J_L/J_w) of PVDF–TiO_2 membranes decreased slightly but was always greater than the ratio (J_L/J_w) of the PVDF membrane. It indicated that the antifouling properties of the PVDF–TiO_2 composite hollow fiber UF membranes were superior to those of the PVDF membrane.

Thermal analysis and mechanical stability of membranes

The thermal analysis results of PVDF–TiO_2 hollow fiber UF membranes are illustrated in Figures 7 and 8, respectively. The thermal decomposition temperature (T_d, defined as the temperature at 3% weight loss) and melting temperature (T_m) of composite membranes increased with the addition of TiO_2 particles when compared with the polymeric membrane. Because of good dispersion and good thermal transmission properties, the TiO_2 particles might strongly hinder the volatility of the decomposed products obtained from pyrolysis and limit the continuous decomposition of PVDF content,[35] thereby enhancing thermal decomposition temperature (T_d). In addition, the restrained state of PVDF chains, owing to the interaction between the macromolecular chain and the polar group on the TiO_2 surface (in this case, hydroxyl), resulted in the enhancement of

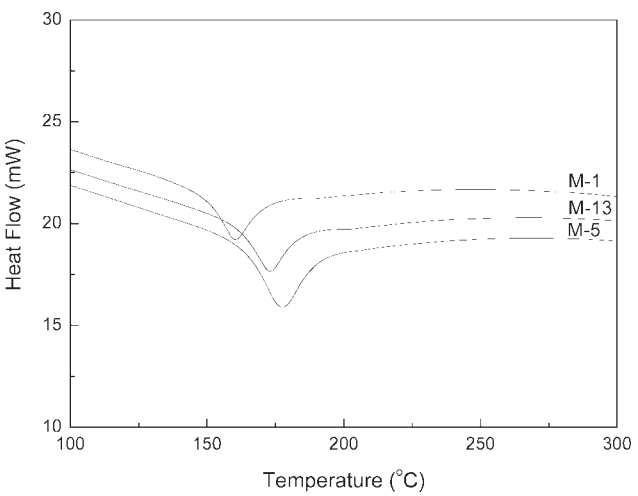

Figure 8 DSC thermograms of PVDF–TiO_2 membranes: M-1, T_m 160.82°C; M-5, T_m 177.27°C; M-13, T_m 173.51°C.

TABLE IV
Mechanical Properties of PVDF–TiO_2 Membranes

Sample number	Tensile strength (MPa)	Elongation at break (%)
M-1	1.71	161.9
M-5	2.26	120.2
M-13	2.16	123.7

the rigidity of polymer chains and restricted their thermal action,[9] thus increasing the melting temperature (T_m) of composite membranes.

In industrial applications of membranes, mechanical properties are very important for long time stable performance. Therefore, the data on tensile strength and elongation at break of hollow fiber membranes were determined. Table IV shows the mechanical properties of PVDF and PVDF–TiO_2 composite membranes. It was clear that the mechanical strength of membranes was enhanced with the addition of TiO_2 particles. The results of TiO_2 particle addition, such as the suppression of macrovoids and the interaction between inorganic particles and polymers, resulted in an increase in the mechanical strength of membranes (M-5 and M-13). However, the tensile strength value of the composite membrane by TiO_2 blending method was less than that of the PVDF–TiO_2 composite membrane by sol–gel method. TiO_2 blending method easily caused particles to aggregate and disperse nonuniformly in the polymer matrix; this formed many stress convergence points in the membrane system under the action of external force, eventually leading to weakening of the mechanical stability of the membrane. Furthermore, rigid inorganic particles in the dope could induce a decline in membrane elasticity, leading to a decrease in the membrane's elongation at break value. Nonetheless, a PVDF hollow fiber membrane containing appropriate amount of TiO_2 particles improved the membrane's mechanical properties, and the tensile strength values were increased by about 30%.

CONCLUSIONS

Organic–inorganic PVDF–TiO_2 composite hollow fiber UF membranes were prepared by the sol–gel method and blending method. The microstructure, hydrophilicity, permeation performance, mechanical properties, and thermal stability of composite membranes were improved apparently by an appropriate choice of TiO_2 concentration. The main conclusions were as follows:

1. Macrovoids were restricted or eliminated, the topical asymmetric structure of membranes became faint and underwent a transition from macrovoids to network pores, and, consequently, the compact resistance of membranes was enhanced.
2. XRD, thermal stability, and mechanical property analyses indicated that interactions between polymers and TiO_2 particles existed. The composite membranes exhibited excellent thermal properties and extraordinary mechanical strength. The mechanical strength of the membrane was enhanced by adding appropriate amount of TiO_2 particles, especially, at 1 wt % TiO_2 by sol–gel method and blending method, and the tensile strength values were increased by about 30%.
3. The composite membranes exhibited extraordinary hydrophilicity and superior permeability with nearly unchanged retention properties compared with the polymeric membrane.
4. Compared with the TiO_2 blending method, the dispersed inorganic network in PVDF–TiO_2 composite hollow fiber UF membranes prepared by TiO_2 sol–gel method and the stronger interaction between inorganic network and polymeric chains led to TiO_2 particles uniformly dispersed in membranes.

References

1. Clarizia, G.; Algieri, C.; Drioli, E. Polymer 2004, 45, 5671.
2. Yang, Y. N.; Wang, P. Polymer 2006, 47, 2683.
3. Guizard, C.; Bac, A.; Barboiu, M.; Hovnanian, N. Sep Purif Technol 2001, 25, 167.
4. Lu, Z. H.; Liu, G. J.; Duncan, S. J Membr Sci 2003, 221, 113.
5. Chiang, P. C.; Whang, W. T.; Tsai, M. H.; Wu, S. C. Thin Solid Films 2004, 447/448, 359.
6. Taniguchi, A.; Cakmak, M. Polymer 2004, 45, 6647.
7. Lang, W. Z.; Xu, Z. L.; Yang, H.; Tong, W. J Membr Sci 2007, 288, 123.
8. Lu, Y.; Yu, S. L.; Chai, B. X.; Shun, X. D. J Membr Sci 2006, 276, 162.
9. Yang, Y. N.; Zhang, H. X.; Wang, P.; Zheng, Q. Z.; Li, J. J Membr Sci 2007, 288, 231.
10. Neoh, K. G.; Tan, K. K.; Goh, P. L.; Huang, S. W.; Kang, E. T.; Tan, K. L. Polymer 1999, 40, 887.
11. Cho, J. W.; Sul, K. I. Polymer 2001, 42, 727.
12. Zoppi, R. A.; Soares, C. G. A. Adv Polym Technol 2002, 21, 2.
13. Honma, I.; Hirakawa, S.; Yamada, K.; Bae, J. M. Solid State Ionics 1999, 118, 29.
14. Kim, J. H.; Lee, Y. M. J Membr Sci 2001, 193, 209.
15. Zhong, S. H.; Li, C. F.; Xiao, X. F. J Membr Sci 2002, 199, 53.
16. Wu, C. M.; Xu, T. W.; Yang, W. H. J Membr Sci 2003, 216, 269.
17. Kim, D. S.; Park, H. B.; Rhim, J. W.; Lee, Y. M. J Membr Sci 2004, 240, 37.
18. Nagarale, R. K.; Shahi, V. K.; Rangarajan, R. J Membr Sci 2005, 248, 37.
19. Cao, X. C.; Ma, J.; Shi, X. H.; Ren, Z. J. Appl Surf Sci 2006, 253, 2003.
20. Bottino, A.; Capannelli, G.; D'Asti, V.; Piaggio, P. Sep Purif Technol 2001, 22, 269.

21. Bottino, A.; Capannelli, G.; Comite, A. Desalination 2002, 146, 35.
22. Lu, Y.; Yu, S. L.; Chai, B. X. Polymer 2005, 46, 7701.
23. Lin, D. J.; Chang, C. L.; Huang, F. M.; Cheng, L. P. Polymer 2003, 44, 413.
24. Zhang, S. Y.; Chen, Z. H.; Li, Y. L.; Wang, Q.; Wan, L.; You, Y. Mater Chem Phys 2008, 107, 1.
25. Xu, Z. L.; Chung, T. S.; Huang, Y. J Appl Polym Sci 1999, 74, 2220.
26. Xu, J.; Xu, Z. L. J Membr Sci 2002, 208, 203.
27. Chung, T. S.; Xu, Z. L. J Membr Sci 1998, 147, 35.
28. Xu, Z. L.; Qusay, F. A. J Membr Sci 2004, 233, 101.
29. McGuire, K. S.; Lawson, K. W.; Lloyd, D. R. J Membr Sci 1995, 99, 127.
30. Li, J. F.; Xu, Z. L.; Yang, H. J Appl Polym Sci 2008, 107, 4100.
31. Li, J. F.; Xu, Z. L.; Yang, H. Polym Adv Technol 2008, 19, 251.
32. Lyster, E.; Cohen, Y. J Membr Sci 2007, 303, 140.
33. McKelvey, S. A.; Koros, W. J. J Membr Sci 1996, 112, 29.
34. Gregorio, R., Jr.; Ueno, J. R. J Mater Sci 1999, 34, 4489.
35. Song, R.; Yang, D. B.; He, L. H. J Mater Sci 2007, 42, 8408.